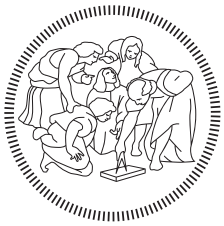

POLITECNICO
MILANO 1863

School of Industrial and Information Engineering

Materials Engineering and Nanotechnology

Materials for Energy

Author
Luigi **Casagrande**

Professor
Silvia **Marola**

Academic Year 2024–2025

Author's preface

Dear Reader,
I am delighted to present this comprehensive collection of lecture notes for ‘‘`Materials for Energy`’’. These notes have been thoughtfully structured to closely align with the course curriculum, providing an invaluable resource for your studies.

These lecture notes are a culmination of extensive research and diligent note-taking, incorporating insights from professor lectures, course materials, textbooks, and other reputable sources. By bringing together these diverse resources, I aimed to provide you with a well-rounded understanding of the subject matter.

While every effort has been made to ensure accuracy and clarity, it is essential to acknowledge that errors or discrepancies may exist within these notes. The complexities inherent in the subject matter, coupled with the limitations of human interpretation, make occasional inaccuracies unavoidable. Therefore, I encourage you to approach these notes critically, supplementing your understanding with additional academic sources and seeking clarification from your professors or peers when necessary.

I have written these lecture notes using LaTeX, a precise typesetting system widely used in scientific and academic writing. Its utilization ensures a visually appealing and organized document, enhancing the overall readability and accessibility of the content.

I sincerely hope that these lecture notes will serve as a valuable companion throughout your academic journey. They are designed to supplement your learning experience, providing a comprehensive overview of the course material. Remember to approach these notes as a guide, actively engaging in discussions, seeking further insights and embracing the collaborative spirit of academia.

Wishing you success and an enriching learning experience.

Milano, Italy
February 6, 2026

Contents

Part I

Theoretical Analysis

1 Introduction

Within the realm of energy materials, the pursuit of efficient and sustainable energy sources remains at the forefront of scientific and technological innovation.
The landscape of energy generation encompasses a diverse array of sources, ranging from conventional fossil fuels to emerging renewable alternatives, each with distinct material requirements and implications.

Note

Fossil fuels, predominantly coal, oil, and natural gas, have long served as the primary energy sources powering global industrialization. However, their finite nature and associated environmental impacts, including greenhouse gas emissions and pollution, underscore the urgency of transitioning towards cleaner alternatives.

Renewable energy sources, including solar, wind, hydroelectric, and biomass, offer promising solutions to mitigate these challenges. Harnessing these resources necessitates advanced materials capable of efficiently capturing, converting, and storing energy. From photovoltaic materials for solar cells to composite materials for wind turbine blades, the development of novel materials plays a pivotal role in enhancing the performance and sustainability of renewable energy systems.

Moreover, the distinction between primary and secondary energy sources underscores the importance of material efficiency in energy conversion processes.
Primary sources, such as sunlight and wind, require materials capable of direct utilization, while **secondary sources**, like electricity, hydrogen or biofuels, demand materials for storage, transmission, and utilization.

Production and **distribution** of energy play critical roles in meeting global demands while considering environmental impacts. Fossil fuel production involves extraction operations such as drilling and mining, often leading to habitat disruption and environmental pollution. In contrast, renewable energy production utilizes resources like sunlight, wind, water, and biomass, each with distinct environmental considerations.
Distribution networks, including the electric grid and pipelines, transport energy from production sites to end-users, necessitating infrastructure maintenance and environmental monitoring.

1.1 Material Efficiency

When choosing materials for energy applications, it's vital to look out for those things:

- Mechanical properties
- Thermal properties
- Electrical properties
- Corrosion resistance
- Chemical compatibility
- Environmental impact
- Cost-effectiveness
- Resource availability
- Lifecycle assessment
- Processing capabilities
- Quality control measures
- Maintenance requirements
- Manufacturing processes

Each of these factors plays a crucial role in selecting materials that meet the performance, reliability, and sustainability requirements of energy systems.

> Material efficiency
>
> **Material efficiency** refers to the effective utilization of materials in a given process or product to achieve the desired outcome while minimizing waste, resource consumption, and environmental impact. It involves optimizing the use of materials throughout their lifecycle, from extraction and processing to manufacturing, use, and disposal.

Material efficiency can be achieved through various strategies, including:

- **Design optimization:** Designing products and processes to use materials more efficiently, such as lightweighting, modular design, and incorporating recyclable or renewable materials
- **Resource conservation:** Conserving raw materials and natural resources by reducing material consumption, reusing materials where possible, and recycling materials at the end of their lifecycle
- **Process improvements:** Implementing more efficient manufacturing processes, such as lean manufacturing, to minimize material waste, energy consumption, and emissions
- **Waste reduction:** Minimizing waste generation through improved material handling, inventory management, and waste recovery or reuse initiatives
- **Life cycle thinking:** Considering the entire life cycle of materials, from extraction and production to use and disposal, to identify opportunities for reducing environmental impacts and resource consumption

The **availability of materials** is a crucial consideration in the selection process for energy applications. It encompasses both the abundance of raw materials and their geopolitical and economic accessibility.
Main factors are:

- **Resource abundance** ▸ Materials required for energy technologies, such as metals, minerals, and rare earth elements, must be sufficiently abundant to support widespread deployment and scalability. Assessing the global reserves and production capacity of these materials helps ensure long-term supply security
- **Geopolitical considerations** ▸ Dependence on materials sourced from geopolitically unstable regions can pose risks to energy security and supply chains. Diversifying material sources and investing in domestic production or strategic partnerships can mitigate these risks
- **Economic factors** ▸ Fluctuations in material prices and market dynamics can influence the cost-effectiveness and viability of energy technologies. Access to affordable materials is essential for achieving competitive energy prices and reducing dependency on volatile markets

Note

The **European Union** identifies certain materials as critical due to their economic importance and supply risk. These critical raw materials, including rare earth elements, cobalt, and graphite, are essential for various high-tech industries, including energy technologies.

2 Strengthening Mechanisms and Conductors

In the design of electrical conductors, especially for overhead transmission systems, material selection must balance electrical conductivity, mechanical strength, cost, and environmental resistance.
This multifactorial optimization is effectively supported by **Ashby selection maps**.

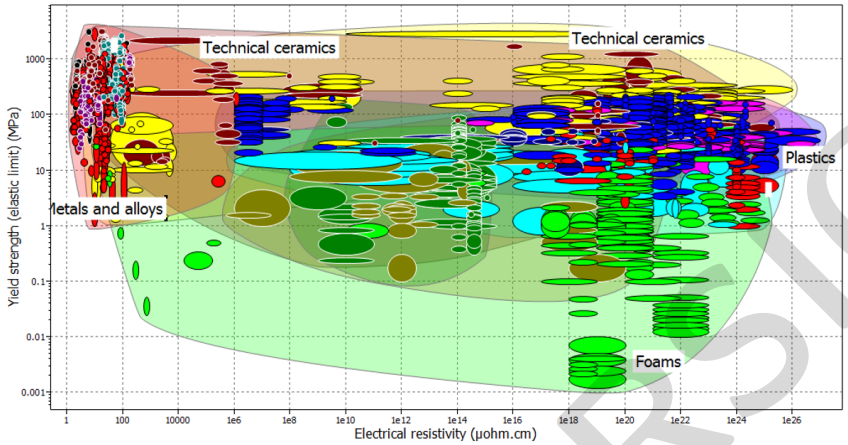

Figure 1: Ashby Map representing Electrical resistivity vs. Yield strength.

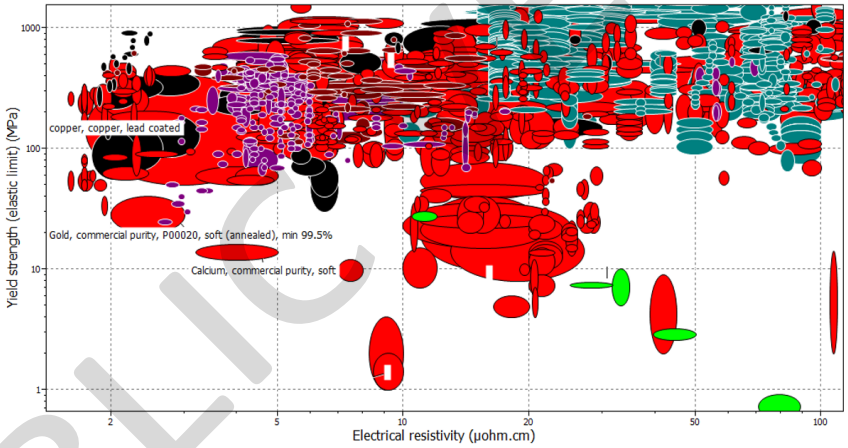

Figure 2: A zoomed-in view of the metals and alloys cluster seen in Figure 1.

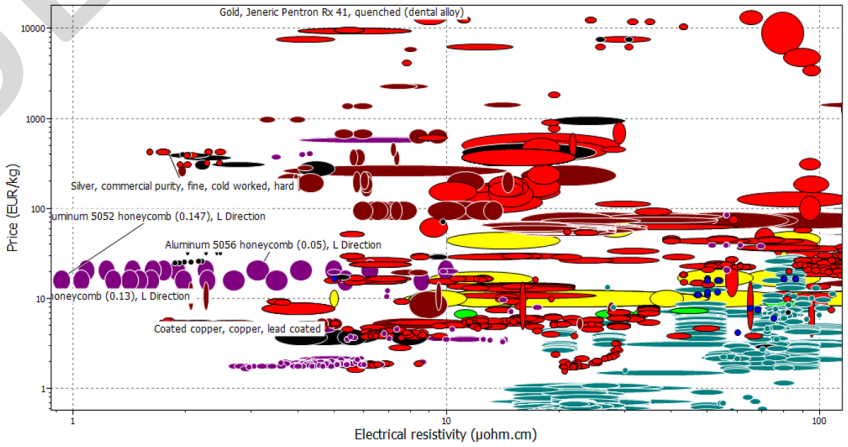

Figure 3: Ashby Map that relates the Electrical resistivity with the material cost.

To enhance the mechanical properties of conductive materials, several strengthening mechanisms are employed. All these methods share a common feature: they **impede dislocation motion**, thereby increasing the yield strength (σ).

Strain Hardening (Work Hardening) ▸ It occurs when a metal is plastically deformed at temperatures below its recrystallization point, increasing the density of dislocations within the crystal lattice. These dislocations interact and entangle, forming barriers that hinder further dislocation glide, thus requiring greater applied stress for continued deformation and resulting in higher yield strength but reduced ductility.

- Common in cold-drawn wires.
- Effect on conductivity: reduces it, due to increased defect-induced scattering.

Grain Refinement ▸ It operates according to the Hall-Petch relationship, which states that decreasing the average grain size increases the number of grain boundaries that act as obstacles to dislocation motion, thereby raising the yield strength and improving toughness by preventing long-range slip.

- According to the **Hall-Petch relation**:

$$\sigma_y = \sigma_0 + \frac{k}{\sqrt{d}}$$

  where σ_y is the yield strength, σ_0 the friction stress, k the Hall-Petch slope (material constant), and d the average grain diameter.

- Effect on conductivity: moderate reduction, as grain boundaries act as scattering centers.

Solid Solution Strengthening ▸ It is achieved by dissolving alloying elements into the host metal to form either substitutional or interstitial solid solutions. The presence of solute atoms introduces lattice distortions due to atomic size or electronic differences, which locally impede dislocation movement by creating stress fields that interact with moving dislocations.

- Effect on conductivity: significant degradation, as solute atoms strongly scatter conduction electrons.

Precipitation (or Particle) Hardening ▸ It involves the controlled formation of finely dispersed, coherent or semi-coherent second-phase particles within the matrix. These precipitates obstruct dislocation motion either by forcing dislocations to bow around them (Orowan mechanism) or by being cut through when sufficiently small, leading to substantial increases in strength and hardness while retaining acceptable toughness.

- Achieved via heat treatment cycles (e.g. T6 for Al alloys).
- Effect on conductivity: depends on volume fraction and coherence; often a compromise.

2.1 Electrical Conductivity

Electrical conductivity [$\mathrm{S\,m^{-1}}$] is a fundamental physical property that quantifies a material's ability to transport electric charge. It is the reciprocal of electrical resistivity, and it is denoted by the Greek letter σ:

$$\sigma = \frac{1}{\rho}$$

where ρ is the electrical resistivity [$\Omega\,\mathrm{m}$].

Note

High conductivity is especially important in materials for electric grids, where power loss due to Joule heating ($P = I^2 \cdot R$) must be minimized.

At the macroscopic level, **Ohm's law** relates voltage V, current I, and resistance R as:

$$\boldsymbol{V = R \cdot I} \tag{1}$$

Resistance $\boldsymbol{R}$ of a conductor with uniform cross-section and length is given by:

$$\boldsymbol{R = \rho \cdot \frac{l}{A}}$$

where l is the length of the conductor, A the cross-sectional area and ρ the resistivity.
Substituting into Ohm's law:

$$\boldsymbol{V = \rho \cdot \frac{l}{A} \cdot I}$$

Thus, for a given material (fixed ρ), the resistance depends purely on geometry.

At the microscopic level, the transport of electricity is due to the motion of free charge carriers, typically electrons in metals.
The **current density $\boldsymbol{J}$** [$\mathrm{A/m^2}$] is defined as:

$$J = \frac{I}{A}$$

The **electric field $\boldsymbol{\xi}$** [V/m] is given by:

$$\xi = \frac{V}{l}$$

The microscopic form of Ohm's Law is then:

$$J = \sigma \cdot \xi \qquad \Rightarrow \qquad \sigma = \frac{J}{\xi}$$

To link this to carrier dynamics, consider a material with free electron density n (carriers/$\mathrm{m^3}$), each of charge $q = -e$, and average drift velocity v_d.
Then:

$$J = n \cdot q \cdot v_d \qquad \Rightarrow \qquad \sigma = \frac{nqv_d}{\xi}$$

This introduces the **mobility of charge carriers $\boldsymbol{\mu}$**, defined as:

$$\mu = \frac{v_d}{\xi} \qquad \Rightarrow \qquad \sigma = nq\mu$$

This result shows that electrical conductivity depends on:

- Carrier concentration n
- Carrier charge q
- Carrier mobility μ

2.1.1 Influence of Structure

In real crystalline solids, electrons are scattered as they move through the lattice. Scattering events reduce both the drift velocity and the mobility.

> **Mean Free Path**
>
> The **mean free path λ** is the average distance an electron travels between two scattering events.

Scattering occurs due to:

- Phonons (thermal vibrations): ↑ with temperature
- Point defects: substitutional or interstitial atoms
- Surfaces and interfaces
- Grain boundaries: interfaces between crystallites
- Second-phase particles and precipitates
- Dislocations: line defects from plastic deformation

Note

These factors reduce μ and hence σ.
Thus any microstructural feature that scatters electrons decreases the conductivity.

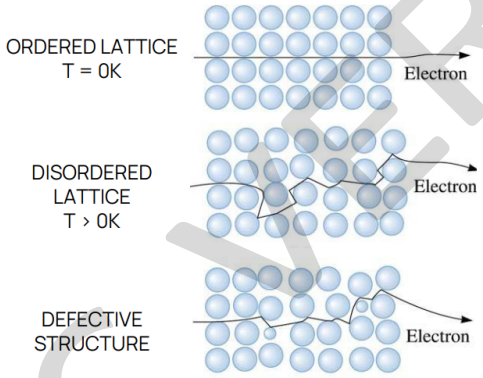

Figure 4

Table 1: How strengthening mechanisms affect electrical conductivity

Strengthening Mechanism	Microstructural Change	Effect on Mean Free Path	Effect on Conductivity
Strain Hardening	Higher dislocation density	Low	Moderate-Strong
Grain refinement	Higher grain boundary area	Low	Mild
Solid solution	Higher solute atoms	Very low	Strong
Precipitation hardening	Higher Second-phase particles	Low	Moderate

This makes it evident that mechanical strengthening is typically **detrimental to electrical conductivity**.

2.2 Electrical Resistivity

While electrical conductivity quantifies the ability of a material to carry electrical current, **electrical resistivity ρ** represents the inherent opposition to charge transport in a given material:

$$\rho = \frac{1}{\sigma}$$

6 Lithium-ion Battery Technology

In the modern era, the demand for efficient, high-performance, and environmentally sustainable energy storage systems has become increasingly critical.
Rapid advancements in portable electronics, electric vehicles, and renewable energy integration have made lithium-ion (Li-ion) batteries the leading technology for electrochemical energy storage.

Li-ion batteries provide several advantages over traditional battery systems, contributing significantly to the reduction of greenhouse gas emissions and the global transition towards renewable energy sources such as solar and wind power.
Unlike fossil fuels, renewable sources are inherently intermittent, and reliable storage solutions are required to balance supply and demand.

6.1 Principles of Electrochemical Energy Storage

> Li-ion Battery
>
> A **Li-ion battery** is a rechargeable electrochemical cell that converts chemical energy into electrical energy through reversible intercalation and de-intercalation of lithium ions between two electrodes: the anode and the cathode.

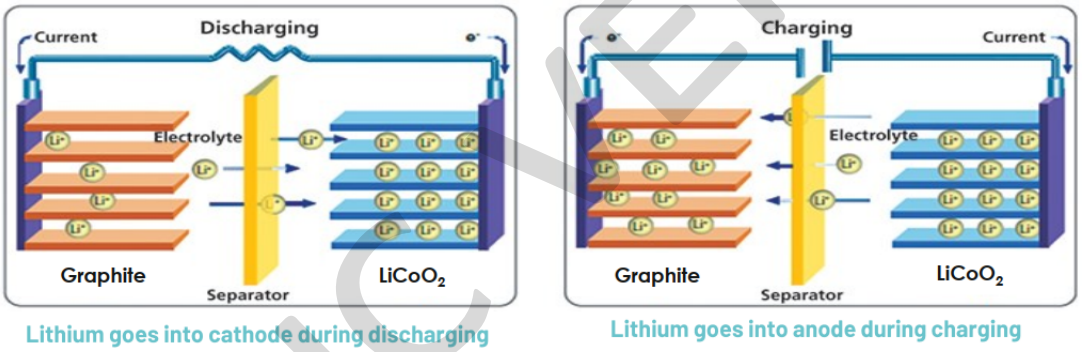

Figure 24

One of the primary advantages of Li-ion technology is its high operating voltage (typically $3.6 - 4.2\,\mathrm{V}$ per cell) and superior energy density, which enable compact and lightweight battery packs with a long operational lifespan exceeding ten years under proper cycling conditions.
Moreover, Li-ion batteries maintain reliable performance across a broad temperature range, generally from -40 to $70\,^{\circ}\mathrm{C}$, making them suitable for diverse environments and applications.

Charge and Discharge Processes

The fundamental working mechanism of a Li-ion battery relies on the **reversible movement of lithium ions and electrons** during charging and discharging.

During **charging**, an external electric field drives lithium ions out of the layered crystal structure of the cathode material, commonly lithium cobalt oxide ($LiCoO_2$).
In this process, cobalt in the cathode undergoes oxidation: cobalt ions transition from an oxidation state of $+3$ to $+4$ by releasing an electron.
This electron travels through the external circuit towards the anode, where the lithium ions are simultaneously intercalated into the anode material, typically graphite, which forms a stable lithium-carbon intercalation compound.

During **discharge**, this process is reversed. Lithium ions migrate back from the graphite anode to the cathode through the electrolyte, while electrons flow through the external circuit, delivering electrical energy to the connected device.

Main Components of a Li-ion Battery

A typical Li-ion battery consists of four primary components:

Anode: The negative electrode, commonly made of graphite, serves as the host for lithium ions during charging.
Alternative materials such as silicon and metallic lithium are under development to enhance energy density.

Cathode: The positive electrode is usually a metal oxide capable of reversibly hosting lithium ions.
Common cathode materials include lithium cobalt oxide (LCO), nickel manganese cobalt oxide (NMC), and lithium iron phosphate (LFP).

Electrolyte: The electrolyte serves as an ionic conductor, allowing lithium ions to shuttle between electrodes while preventing electronic conduction within the cell. Liquid electrolytes typically consist of a lithium salt dissolved in a mixture of organic solvents.
Widely used lithium salts include lithium hexafluorophosphate ($LiPF_6$), lithium bis(fluorosulfonyl)imide (LiFSI), and lithium bis(trifluoromethanesulfonyl)imide (LiTFSI).
Common solvents include ethylene carbonate (EC), fluoroethylene carbonate (FEC), ethyl methyl carbonate (EMC), and dimethyl carbonate (DMC). Carefully selected additives improve thermal stability, cycling performance, and the formation of a stable solid electrolyte interphase (SEI) layer on the anode.

Separator: The separator is a porous polymer membrane that prevents physical contact between the cathode and anode, avoiding internal short circuits. It also acts as an electrolyte reservoir, enabling ionic transport.
Typical separators are based on polyethylene (PE) and polypropylene (PP), often arranged in PP/PE/PP trilayer configurations and sometimes coated with ceramic materials to enhance thermal stability and mechanical integrity over a broad temperature range.

Electrode Materials: Cathodes and Anodes

The choice of electrode materials critically influences the overall performance, cost, and safety of Li-ion batteries.

Cathode Materials:

- **LCO** ($LiCoO_2$): High energy density, widely used in portable electronics but expensive and less thermally stable at high states of charge.
- **NMC** ($LiNi_xMn_yCo_zO_2$): Offers a balanced compromise between energy density, cost, and thermal stability; commonly used in electric vehicles.
- **LFP** ($LiFePO_4$): Provides excellent thermal and chemical stability, lower energy density but enhanced safety and longer cycle life.

Anode Materials:

- **Graphite:** The conventional anode material with a theoretical specific capacity of 372 mAh/g. Although robust and well-established, graphite's limited lithium storage capacity and relatively high carbon footprint motivate the search for alternatives.

- **Silicon:** Emerging as a promising alternative due to its exceptionally high theoretical specific capacity ($\sim 3000\,\mathrm{mAh/g}$), which is nearly ten times that of graphite. Silicon can theoretically host about 4.4 lithium atoms per silicon atom, enabling thinner, lighter, and more energy-dense cells.
  However, silicon anodes suffer from significant challenges such as volumetric expansion during cycling, which leads to pulverization, delamination, and instability of the SEI layer.
- **Pure Lithium Metal:** Provides the highest theoretical capacity among anode materials but is limited by safety risks such as dendrite formation, which can cause internal short circuits. Moreover, lithium's low melting point ($180\,^{\circ}\mathrm{C}$) and its soft nature further complicate practical implementation.

Electrolyte

The electrolyte plays a central role in defining a battery's cycle life, energy density, power capability, and safety. The optimal electrolyte must exhibit high ionic conductivity, wide electrochemical stability, low flammability, and excellent compatibility with both electrode materials. Research is actively exploring solid-state electrolytes and advanced liquid formulations to mitigate safety risks such as thermal runaway and flammability associated with conventional organic electrolytes.

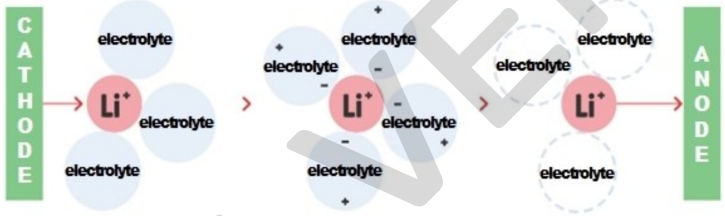

Figure 25

Separator

An effective separator must maintain mechanical strength, thermal stability, and chemical compatibility with the electrolyte under demanding operating conditions.
Modern separators employ multilayer structures and ceramic coatings to suppress shrinkage and maintain structural integrity under high temperatures, which is critical for preventing catastrophic short circuits.

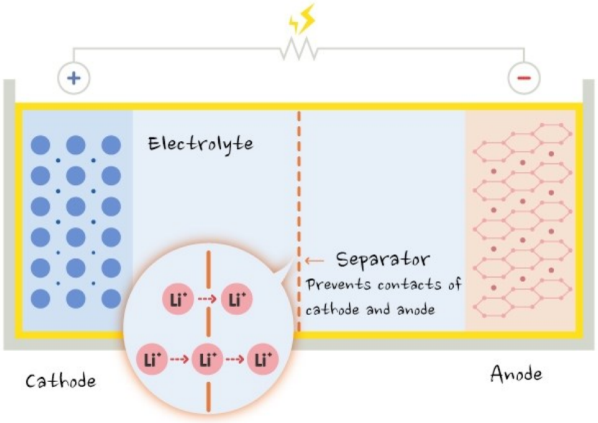

Figure 26

Part II

Case Study

1 Failure of an overhead conductor

The failure of the overhead conductor crossing the Paraná River serves as a case study that underscores the strategic importance of robust material selection and engineering design in critical infrastructure.
As one of South America's major waterways, the Paraná River presents numerous technical challenges for overhead conductor systems, including long span requirements, strong hydrodynamic forces, extreme weather conditions, and potential corrosion from humid or chemically aggressive environments.

The collapse of this cable crossing had severe consequences, ranging from regional blackouts and transport disruption to increased economic losses and compromised public safety. This event highlights the systemic interdependence between infrastructure reliability and socio-economic stability, emphasizing the need for rigorous materials engineering and failure prevention strategies.

Designing overhead conductors for river crossings – particularly across large and dynamic systems like the Paraná River – requires a delicate balance of multiple performance criteria.
Key engineering challenges include:

- Mechanical Loading: Long spans experience significant tensile stresses, both from the weight of the conductor and external forces such as wind and ice loading
- Sag Control: Excessive sag can reduce ground clearance and increase the risk of mechanical failure or electrical arcing
- Thermal Expansion: High current loads generate Joule heating, which must be controlled to prevent dimensional instability
- Corrosion Resistance: Proximity to water bodies and high humidity levels increase the risk of galvanic or pitting corrosion
- Electrical Efficiency: High conductivity is essential to minimize energy losses over long distances
- Cost Optimization: Economic considerations impose constraints on material selection and manufacturing complexity

Table 2: Primary design objectives for overhead conductors

Functional Requirement	**Target Material Property**
Lightweight for long spans	Low density
Efficient power transmission	High electrical conductivity
Dimensional and mechanical stability	High tensile strength, high Young's modulus, low thermal expansion
Environmental durability	High corrosion resistance
Cost-effective deployment	Low raw material and processing cost

Several materials are employed in overhead conductor systems, often in composite configurations to meet multifaceted performance demands.

COPPER is historically one of the first materials used for electrical conductors due to its superior electrical conductivity ($\sim 58\,\mathrm{MS/m}$) and good mechanical strength. It also exhibits excellent corrosion resistance in most atmospheric conditions.

However, copper's high density ($\sim 8.96\,\mathrm{g/cm^3}$) increases the weight of the conductor, which can lead to higher mechanical stress and increased sag in long-span applications.
Furthermore, copper is significantly more expensive than aluminum, limiting its use in large-scale transmission lines.

Note

It is therefore primarily used in short-span or high-reliability segments where conductivity and thermal stability are paramount.

ALUMINIUM is the most commonly used material for overhead transmission lines.
It offers a favorable combination of:

- Low density ($\sim 2.70\,\mathrm{g/cm^3}$) → reduces mechanical loading
- High electrical conductivity ($\sim 35\,\mathrm{MS/m}$, $\sim 61\,\%$ that of copper) → efficient transmission
- Excellent corrosion resistance → protective oxide layer forms naturally
- Cost efficiency → lower cost per unit weight than copper

Its moderate mechanical strength is typically augmented through alloying or by incorporating a steel core.

STEEL is primarily used as a reinforcement core in Aluminum Conductor Steel Reinforced (ACSR) cables. It provides:

- High tensile strength → suitable for long spans and heavy mechanical loading
- Structural rigidity → minimizes sag and mechanical deformation
- Moderate cost

However, steel is electrically conductive but inefficient for power transmission, and is prone to corrosion unless galvanized or coated. Its use is therefore limited to structural support, not as a current-carrying medium.

1.1 Engineering Considerations

When designing an overhead conductor crossing a major river such as the Paraná, the most critical mechanical constraint is the long span between supporting towers. The conductor must carry its own weight over this distance without intermediate supports, resulting in high tensile stresses and increased sag, which must be controlled to maintain safety and performance standards.

In addition to mechanical demands, the proximity to the river introduces environmental challenges. Persistent humidity and exposure to water vapor can accelerate **corrosion**, particularly in areas where protective coatings degrade or where dissimilar metals are in contact, potentially triggering galvanic processes. Over time, such degradation can compromise both the electrical and structural integrity of the system, leading to premature failure.

1.2 Failure Analysis

> Failure Analysis
>
> **Failure analysis** is the systematic investigation of a failed component to determine the cause, mechanism, and contributing factors behind its breakdown. In the context of engineering infrastructure, it serves both a preventive and forensic function.

Technically, it enables the identification of failure modes such as overload, fatigue, or corrosion. Legally, it can help assign responsibility in the event of litigation or insurance claims. From a design perspective, it provides data necessary for improving future implementations and preventing recurrence under similar service conditions.

A complete failure analysis typically begins with a visual inspection of the installation site, noting environmental conditions and structural context. It continues with a reconstruction of the events leading up to the failure, including mechanical loads, environmental exposure, and electrical operating conditions.
Finally, the physical remnants of the failed component are examined – often using microscopy or spectroscopic techniques – to characterize the fracture surface, identify signs of corrosion or fatigue, and detect possible manufacturing defects.

In the case of the Paraná River conductor failure, a visual inspection was performed on the damaged cable. A cross-sectional view (Figure 40) revealed a concentric arrangement of outer and inner strands, typical of ACSR (Aluminum Conductor Steel Reinforced) design.

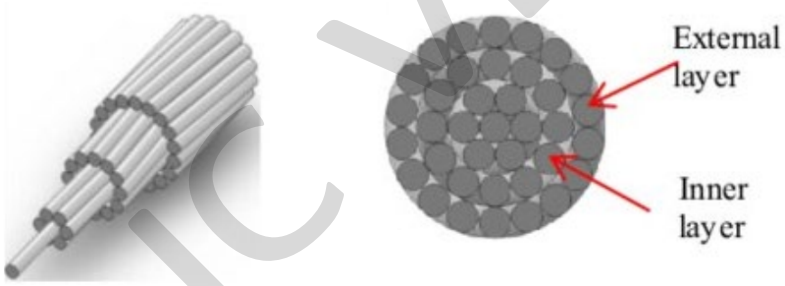

Figure 40: Cross-section view of the cable.

The outer layer consisted of high-conductivity aluminum, while the inner core, as shown in Figure 41, was made of high-strength steel used to bear mechanical loads over the long span.

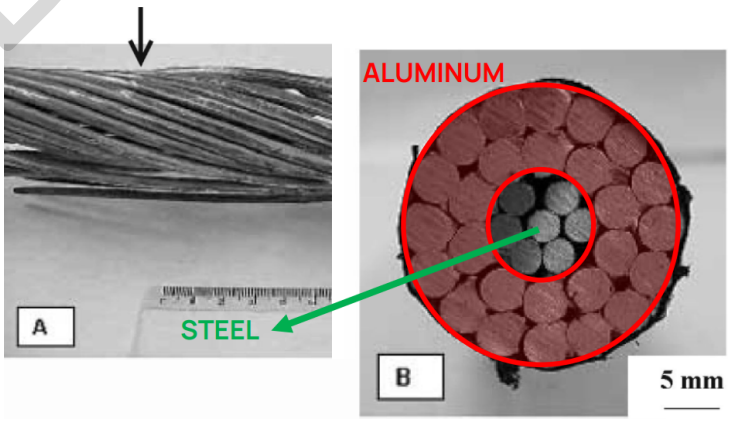

Figure 41

The fractured region, illustrated in Figure 42, exhibited characteristics that offer insight into the

failure mechanism. If the fracture surface appeared granular and clean, it would suggest a brittle fracture, possibly caused by sudden overload or material embrittlement. In contrast, features such as necking, radial marks, or corrosion pits could point to ductile failure, progressive fatigue, or corrosion-assisted cracking.

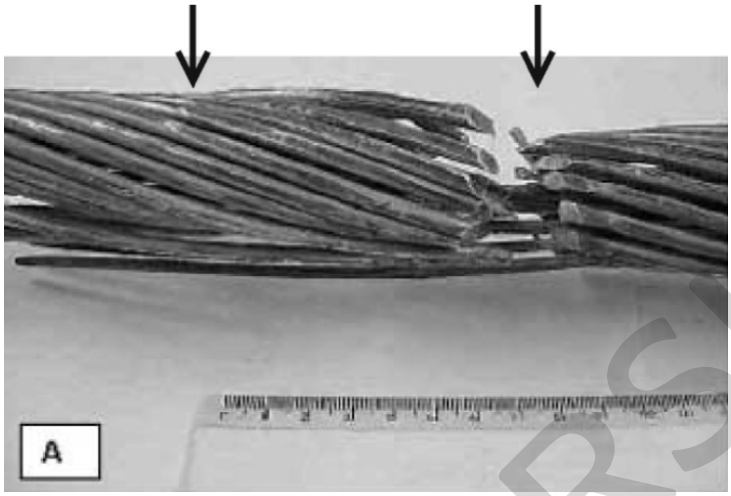

Figure 42: Fractured region.

1.2.1 Location and Morphology of the Failure

The failure was localized in the **clamped region** of the overhead conductor.
Clamps are critical mechanical components used to maintain the relative position of adjacent conductors and to prevent contact that could cause electrical arcing or mechanical interference.

Figure 43: Clamps placements.

In this case, the failure occurred precisely where the conductor was held in place by a spacer clamp – a mechanically constrained region that is subject to both static loading and micro-movements due to thermal cycling and mechanical vibrations.

Visual inspection of the fracture surface (Figure 44) revealed a characteristic 45° fracture angle in the outer aluminum strands, consistent with shear-dominated failure. Toward the central region,

the fracture became more normal to the axis ($\sim 90^\circ$), indicating a different stress regime in the steel core. The space between the two failure zones corresponded to the physical position of the clamp, suggesting a mechanical incompatibility or fatigue accumulation at the conductor-clamp interface.

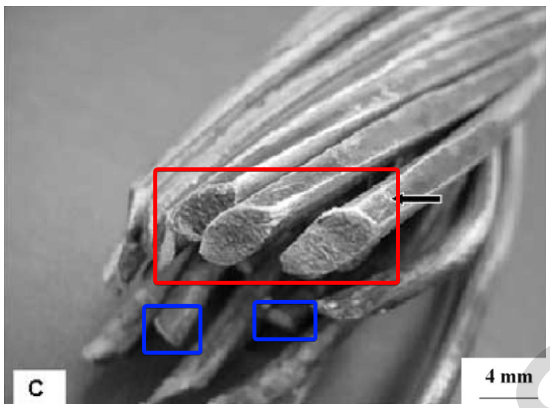

Figure 44

1.2.2 Clamp Design and Wear Analysis

The clamp responsible for securing the conductor – specifically, Spacer Clamp No. 4 (Figure 45) – is a nut-cracking type made from a cast Al-10%Si alloy. It consists of two pivoting half-cylinders that enclose the cable and are mechanically fastened by a steel bolt screwed into a threaded socket in the lower clamp body.

Note

This configuration is designed to provide uniform radial compression and secure mechanical contact.

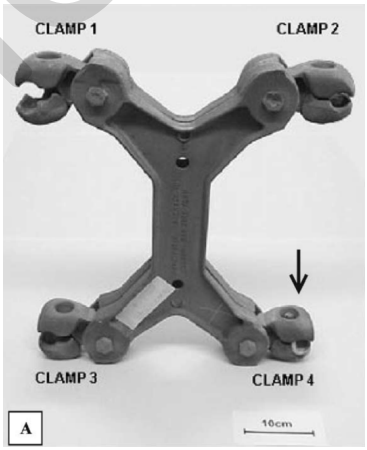

Figure 45: Clamp design.

However, severe wear was observed on the internal surface of the clamp, with a material loss of approximately 2 mm (Figure 46). The wear had progressed to the point of exposing the steel fixation bolt, indicating that the aluminum surface had been eroded through persistent contact. This reduction in clamp-conductor interface integrity led to a significant drop in contact pressure, which in turn allowed greater relative displacement between the two surfaces.
Such displacement is characteristic of a **fretting regime**, where small oscillatory motions under

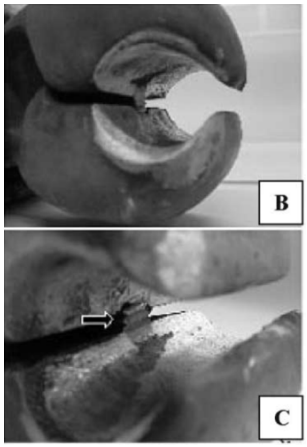

Figure 46: Clamp No. 4

normal load generate surface damage, oxide debris, and progressive wear. Once fretting initiates, the system enters a self-reinforcing cycle of micro-movement, surface degradation, and mechanical fatigue, ultimately leading to structural failure.

1.2.3 Surface Markings and Fretting Indicators

Further inspection of the clamp's interior surface revealed two distinct types of wear markings, each indicative of specific mechanical interactions:

- **Oriented dark bands** (indicated by white arrows in the visual documentation) are attributed to static contact marks. These are likely caused by plastic deformation during initial tightening or by the prolonged presence of entrapped particles between the conductor's outer strands and the clamp's inner surface. Their alignment with the strand geometry supports this interpretation.
- **Circumferential wear lines** (highlighted by black arrows) correspond to dynamic fretting marks. These features align with the direction of relative motion and provide clear evidence of micro-slip between the clamp and the cable. Their presence confirms that the mechanical contact had transitioned from a static hold to a dynamic interaction, consistent with a critical fretting regime.

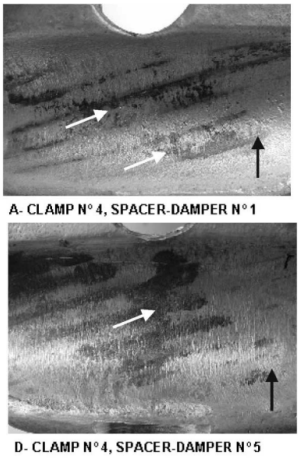

Figure 47

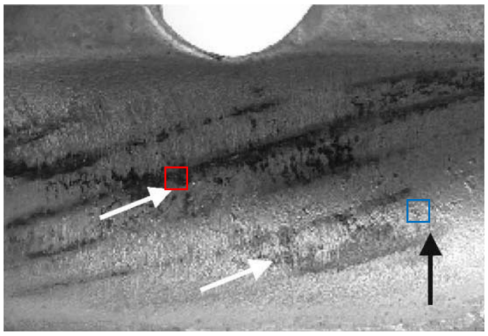

Figure 48

Detailed visual inspection of Figure 48 highlights the presence of two distinct wear features on the aluminum strands at the conductor-clamp interface:

- **Static marks**, highlighted in red, exhibit a darker coloration due to accumulated debris. These form in regions of prolonged, stationary contact between the aluminum strands and the clamp, especially under corrosive environmental conditions where humidity accelerates degradation.
- **Dynamic marks**, shown in blue, consist of circumferential wear patterns and transversal microcracks. These are clear signatures of fretting, a surface damage mechanism driven by small-amplitude oscillatory movements between contacting components under load.

On both the outer and inner aluminum strands, **narrow rectangular static marks** were observed precisely at the strand-strand contact zones. Ideally, the contact between layers should be point-like, resulting in highly localized pressure.
However, due to relative displacement and plastic deformation, the contact area evolves into elliptical wear patterns. These deformed zones concentrate stress and promote debris accumulation.

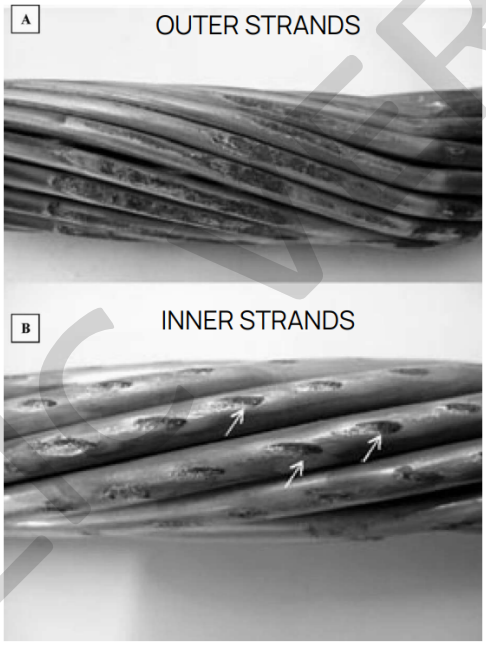

Figure 49

Particularly severe plastic deformation and surface wear were detected in the inner strands (Figure 49), especially just ahead of the clamp region – a mechanically critical transition zone where the relative motion between aluminum layers increases while the restraining pressure from the clamp diminishes.

Note

All these dark wear features were characterized by embedded debris, indicating active material loss and surface interaction under mixed loading conditions.

1.2.4 Debris Composition

Chemical and mechanical analysis of the wear debris provided further insight into the fretting environment:

- On the outer aluminum strands, two distinct types of particles were found:
  - **Aluminum oxide** (Al_2O_3) particles within the tangential wear marks. These are highly abrasive, with a hardness of ~ 2000 HV, and form due to oxidative wear under cyclic contact.
  - **Silicon dioxide** (SiO_2) particles on the strand's external surfaces in regions of contact with the clamp. Their hardness ranges from 800 to 1400 HV, and their presence suggests contamination from environmental sources or third-body abrasion.
- On the inner aluminum strands, only Al_2O_3 particles were identified, again concentrated within the fretting paths.

The high hardness and abrasive nature of these particles further accelerated surface damage and material removal during fretting.

1.3 Mechanical Service Conditions and Failure Mechanisms

Overhead conductors operate under complex loading environments, especially near clamping points where both static and dynamic effects contribute to degradation.

- **Geometric stress concentration** occurs at the clamp due to curvature constraints and localized compression.
- **Static contact stresses** arise from:
  - the cable's self-weight and axial load over the span,
  - bending moments imposed by the clamp's geometry,
  - and direct clamping pressure applied by the device.

In parallel, cyclic stresses are induced by environmental factors – primarily **wind-induced vibrations**, which cause alternating bending and movement at the contact interface.
These oscillations may persist over tens of millions of cycles, triggering:

- Fatigue failure of aluminum strands,
- Fretting fatigue, where micro-slip and high-cycle stress combine to initiate cracks and remove material.

Additionally, mechanical tension along the conductor axis induces an **internal torque**, which tends to **unwind** the stranded geometry. Any tension fluctuation can excite **torsional vibrations**, transferring torque to the clamp interface. Depending on the effectiveness of the clamping force, the conductor may rotate within the clamp, increasing the risk of fretting damage through tangential displacement.

Note

This interaction between tension, rotation, and movement fosters complex fretting-fatigue mechanisms that can significantly reduce the service life of the conductor.

Finally, **galvanic corrosion** was observed between the aluminum strands and steel elements (zinc-coated) within the clamp. This electrochemical process is exacerbated in industrial or marine atmospheres, where moisture and contaminants accelerate corrosion.

In typical high-performance conductor systems, **grease filling**[4] is applied between strands to block the ingress of aqueous corrosives and inhibit galvanic interaction. However, in this case, no grease was used, exposing the aluminum to both mechanical wear and electrochemical attack.

1.4 Metallurgical Analysis of the Spacer Clamp

The spacer clamp under investigation is manufactured from an Al-10%Si hypoeutectic aluminum-silicon alloy, a common material in casting applications due to its good castability and wear resistance. The component was produced through a traditional foundry process, implying relatively slow cooling rates and limited microstructural control.

By analyzing a cross-sectional view of the clamp, two key aspects can be examined:

- The **bulk microstructure**, revealing the solidification features of the alloy
- The **surface layer**, where wear damage and material detachment are evident due to service conditions

1.4.1 Al-Si Casting Alloys

In the Al-Si binary system, the eutectic composition occurs near 12.6 wt% Si. At 10 wt% Si, the alloy is hypoeutectic, meaning it solidifies with primary α-Al dendrites, followed by the formation of a (Al + Si) eutectic upon further cooling.

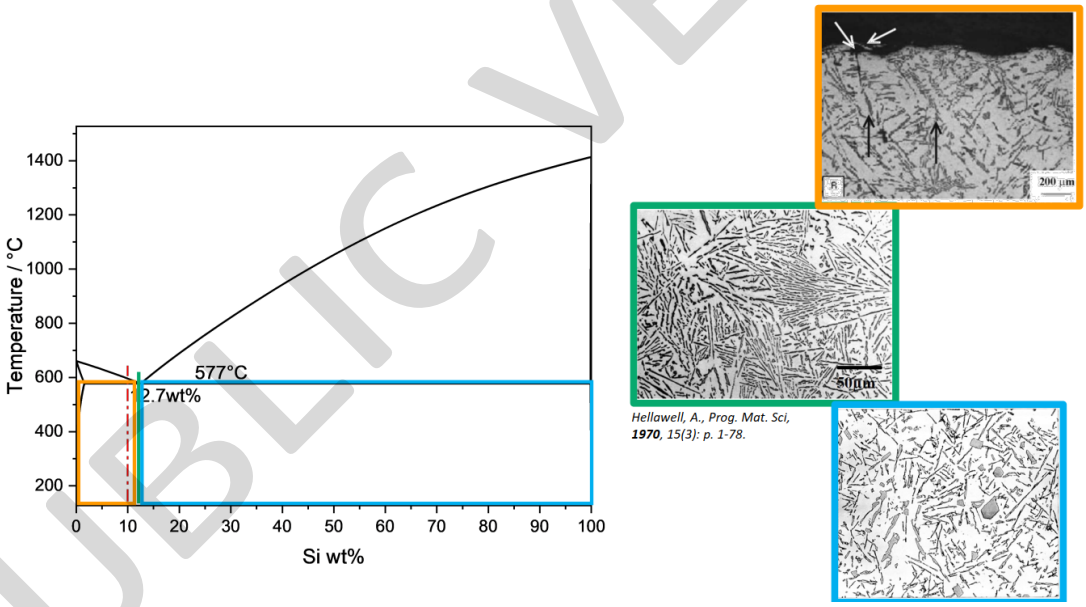

Figure 50

A typical phase diagram shows that even small changes in Si content near 2.7 wt% can lead to the coexistence of three solid phases during solidification, affecting the alloy's morphology and mechanical response.

The cooling rate during casting plays a crucial role in determining the size and morphology of the eutectic phase:

[4] A grease filling is a lubricant composed of oil ($70-90\,\%$) thickened with a soap (e.g., lithium, calcium) or synthetic thickener, plus additives (anti-wear, corrosion inhibitors). It's made by dispersing the thickener in oil under heat, then cooling to form a semi-solid.

- **Higher solidification rates** produce finer eutectic structures, with improved mechanical behavior
- **Lower cooling rates** lead to coarser Si lamellae, often irregularly distributed, and prone to crack initiation under load
- These microstructural differences directly influence the alloy's hardness, ductility, and fatigue strength

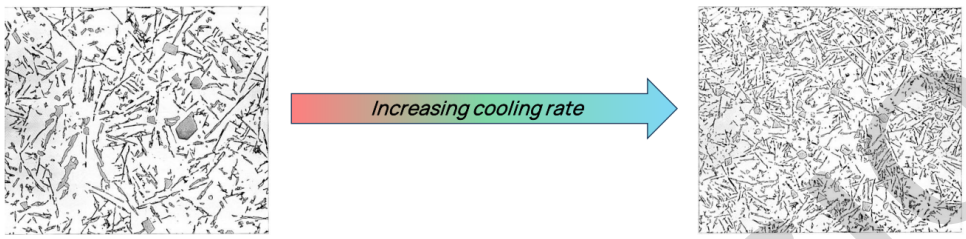

Figure 51

The mechanical performance of Al-Si casting alloys can be significantly enhanced through eutectic modification:

- Minor additions of elements such as **sodium** (Na) or **strontium** (Sr) transform the Si morphology from plate-like lamellae to a coral-like fibrous network.
- This **modified microstructure** (Figure 52) results in:
  - Higher ductility
  - Improved ultimate tensile strength (UTS)
  - Increased hardness
  - Better fatigue resistance, particularly under cyclic or fretting conditions

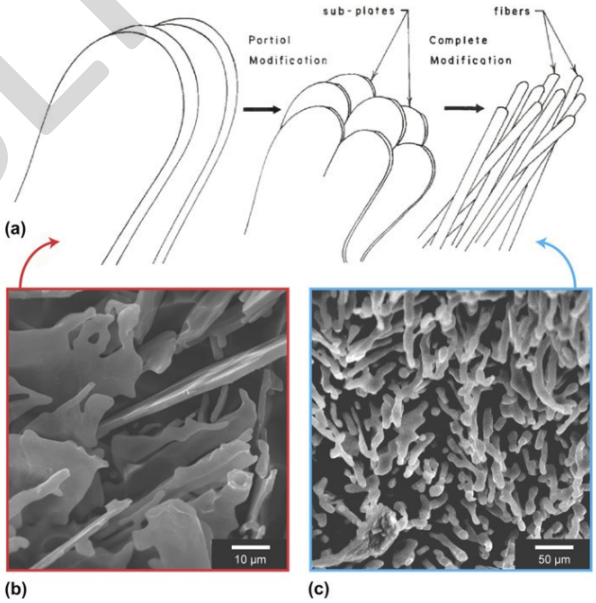

Figure 52

Returning to the clamp, the observed microstructure confirms:

- A slow-cooled, unmodified Al-10%Si alloy
- Coarse eutectic silicon lamellae heterogeneously distributed throughout the matrix
- No evidence of eutectic modification elements being used

This unrefined structure makes the clamp vulnerable to **mechanical degradation**:

- Under high shear or contact stresses, decohesion can occur at the Al/Si interfaces
- Resulting in material removal, surface cracking, and reduction of effective clamping pressure

The measured macrohardness of the component was 63 HV, consistent with expectations for a cast, unmodified Al-10%Si alloy.

Note

To enhance the mechanical reliability of future components, a modified eutectic structure should be considered. This can be achieved through alloying additions and controlled solidification, improving both wear resistance and toughness under service conditions.

1.5 Analysis of Fixation Bolts and Clamping Interface

The spacer clamp is secured using fixation bolts made of **SAE 1008 low-carbon steel**, a material known for its good formability and weldability. Metallographic inspection reveals a low pearlite content, with pearlite colonies aligned along the vertical axis, indicative of hot plastic deformation during rod production.

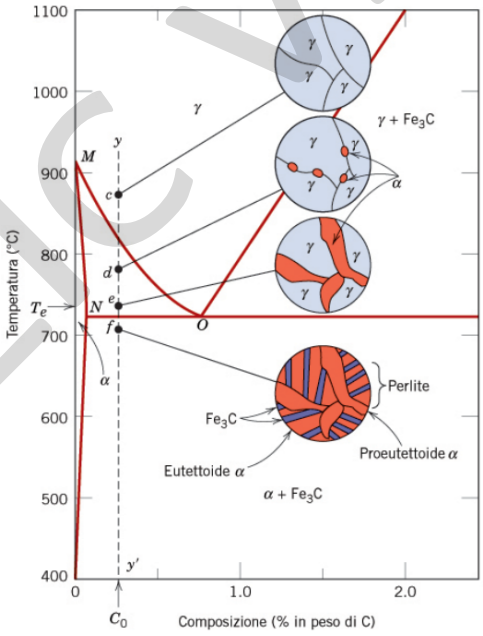

Figure 53

Closer to the thread region, microstructural differences confirm that the threads were formed by cold plastic deformation rather than machining. This is consistent with standard bolt manufacturing processes, which enhance thread strength via work hardening.

- **Core hardness:** 156 HV
- **Surface treatment:** Visual evidence suggests a zinc-plated surface, commonly used for corrosion protection in steel fasteners exposed to atmospheric conditions.

4.7 Case Study III: Creep and Creep Rupture of Parts Having Complex Geometries

Modern **steam power plants** operate under severe thermal and mechanical loading conditions which place stringent demands on the high-temperature performance of structural components. Among the principal degradation mechanisms encountered in such environments, creep – the time-dependent plastic deformation of materials under constant stress at elevated temperatures – remains one of the most critical, as it ultimately governs the service life and safety of essential components.

A defining aspect of engineering design for creep resistance lies in the fact that most real-world components possess complex geometries.
Geometrical features such as notches, holes, grooves, welds, and abrupt changes in cross-sectional area act as local stress concentrators, significantly influencing how creep damage initiates and propagates.
Therefore, understanding creep and creep rupture in parts with non-uniform shapes is fundamental for the reliable design and assessment of high-temperature equipment.

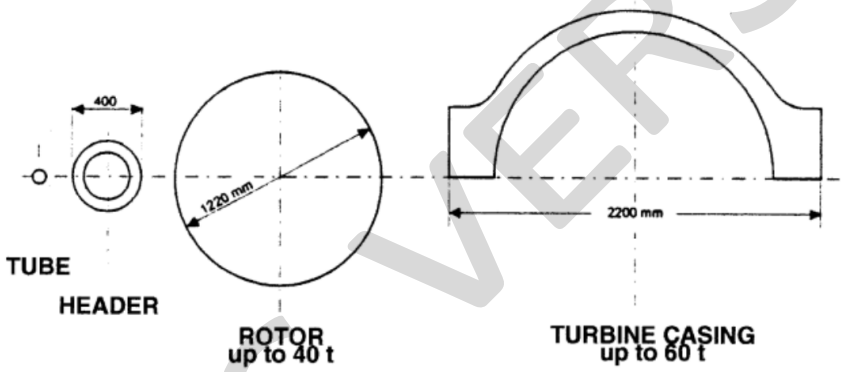

Figure 94

To illustrate the scale and structural challenges, consider the typical dimensions of major components in modern steam turbines:

- **Headers** often have diameters of around 400 mm
- **Rotors**, which must endure high rotational speeds and thermal gradients, can weigh up to 40 tonnes, with diameters reaching 1220 mm
- **Turbine casings**, enclosing the rotor assemblies and controlling steam flow, are even larger, with weights up to 60 tonnes and diameters of approximately 2200 mm

These large-scale components are subjected to varied service conditions, which require careful selection of materials with tailored properties to withstand their specific mechanical and thermal loads.

Material Requirements for Different Components

Within a steam turbine, different sections experience distinct stress states and thermal regimes:

- **High-pressure/intermediate-pressure (HP/IP)** and **low-pressure (LP)** sections use different steels to balance creep strength, toughness, and other performance criteria.
- **Rotors** and **blades** are subjected to significant centrifugal stresses due to rotation and

require materials with high creep rupture strength, fatigue resistance, and stable microstructure under thermal cycling.

- By contrast, **vents**, **casings**, and **housings** typically experience no rotational stresses but must still withstand internal pressures, thermal expansion, and possible thermal fatigue.

For **low-temperature (LT) turbine components** – or parts that operate at temperatures below the creep range – other material properties can become more significant than creep resistance.
For example, fracture toughness, Ultimate Tensile Strength (UTS), weldability, and wear resistance are often prioritized to ensure structural integrity and ease of fabrication or maintenance.

Creep Rupture Mechanisms in Components with Complex Geometries

Experimental investigations of creep rupture are commonly carried out on axially loaded specimens, either smooth or deliberately notched to replicate stress concentrations similar to those found in service components.
Observations from such tests reveal multiple modes of creep damage:

- **Diffuse creep damage**, characterized by a uniform distribution of cavities and microvoids throughout the material, typically seen in smooth specimens.
- **Localized creep damage**, which occurs preferentially in regions of stress concentration, such as the root of a notch, weld toes, or geometrical transitions.
- **Formation and propagation of creep cracks**, which initiate from sites of severe damage coalescence and progress under the combined influence of creep deformation and stress intensification.

Experimental figures illustrating these mechanisms often depict micrographs showing cavity nucleation and growth, as well as macro-scale fracture surfaces displaying characteristic creep crack paths.

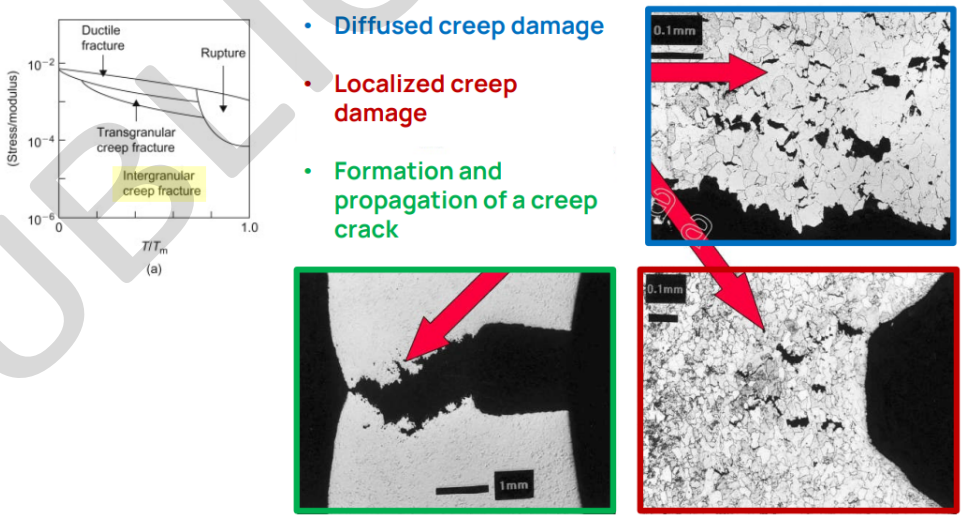

Figure 95

Notched Specimens as Idealized Models for Complex Geometries

To systematically study the influence of stress concentrations, notched cylindrical specimens are widely used.

The geometry of these specimens can be defined by several key parameters:

- The **notch radius**, denoted by R, which dictates the sharpness of the stress concentration.
- The **diameter** or **radius of the unnotched section**, denoted by b.
- The **minimum diameter** or **radius at the notch root**, denoted by a.

The **notch acuity ratio**, given by $\boldsymbol{a/R}$, is a dimensionless measure of the notch sharpness – the smaller the radius R relative to a, the sharper the notch and the higher the stress concentration.

Figure 96

The local net stress in the minimum cross-sectional area can be approximated as:

$$\sigma_{\text{net}} = \frac{\sigma_0}{A_{\min}} = \frac{F_y}{A_{\min}}$$

For example, for a given applied force F_y and minimum cross-sectional area $A_{\min}$, the net section stress might reach values such as 290 MPa, which then serves as the reference stress for creep rupture calculations.

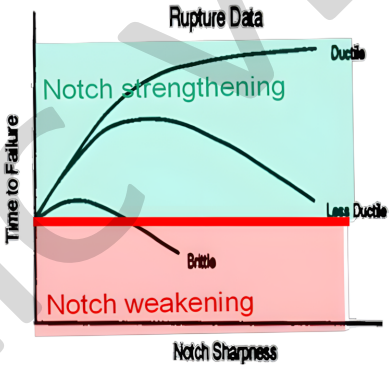

Figure 97

Influence of Notches on Creep Strength

The presence of a notch alters the stress state within a component and influences both the creep strength and rupture time.
Two important parameters are used to quantify this effect:

- The **Notch Strength Ratio (NSR)** compares the rupture stress of a notched specimen (σ_N) to that of an equivalent smooth specimen (σ_S) tested under the same rupture time:

$$\text{NSR} = \frac{\sigma_N}{\sigma_S} \quad \text{(constant rupture time)}$$

- The **Notch Time Ratio (NTR)** compares the rupture time of a notched specimen (τ_N) to that of a smooth specimen (τ_S) under the same nominal stress:

$$\text{NTR} = \frac{\tau_N}{\tau_S} \quad \text{(constant stress)}$$

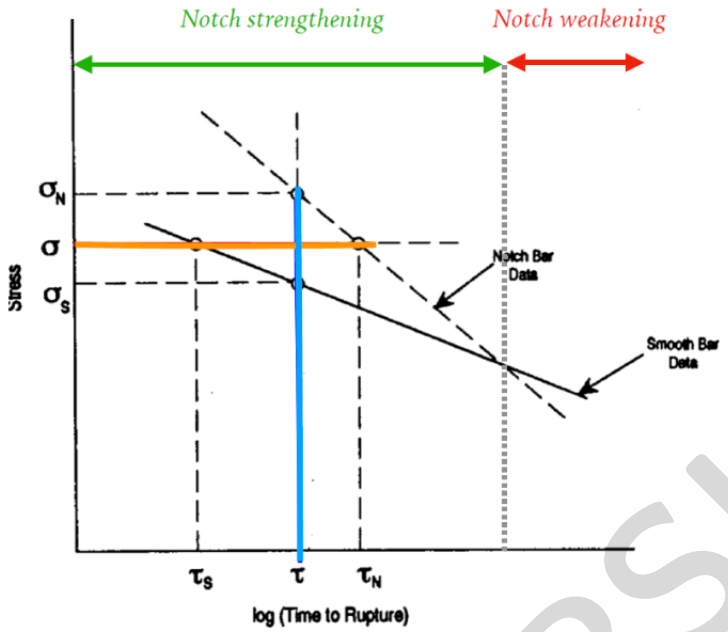

Figure 98

Interestingly, notches do not always weaken a component in creep. Due to stress redistribution by local plasticity and creep relaxation, notched specimens can sometimes exhibit an apparent strengthening effect, a phenomenon known as notch strengthening.

This effect arises because stress redistribution leads to triaxial stress states that inhibit cavity growth and crack propagation compared to smooth specimens, thereby extending rupture life in certain conditions.

A defining feature of creep deformation in parts with stress concentrators is **stress relaxation**. Initially, the stress at the notch root is very high due to the sharp geometry. Over time, creep deformation redistributes the local stress field, reducing the peak stress and transferring load to adjacent regions.
This behaviour is crucial in practice because it explains why local stress intensities do not always lead to immediate failure but rather evolve gradually during service.

Experimental plots typically depict **equivalent stress versus time** for a notched specimen under constant load. These curves clearly show the decay of peak stress due to creep strain accumulation and redistribution.

Note

A thorough understanding of creep rupture in components with complex geometries enables engineers to design steam plant parts with reliable long-term performance.
It allows for appropriate material selection, informed notch design, the introduction of fillets or gradual transitions to mitigate stress concentrations, and the use of weld geometries and post-weld treatments that minimize localized creep damage.

Moreover, by interpreting test results for notched and smooth specimens, engineers can develop life assessment models that better predict how real components – far more geometrically complex than idealized test bars – will behave under prolonged high-temperature service.

Experimental Local Creep Strain

When studying the creep behaviour of structural components, it is fundamental to recognize that the distribution of strain within a component is rarely uniform, especially in the presence of geometrical discontinuities, notches, welds, or abrupt changes in cross-sectional area.
Experimental investigations of local creep strain provide essential insight into how deformation localizes and evolves over time under service conditions.

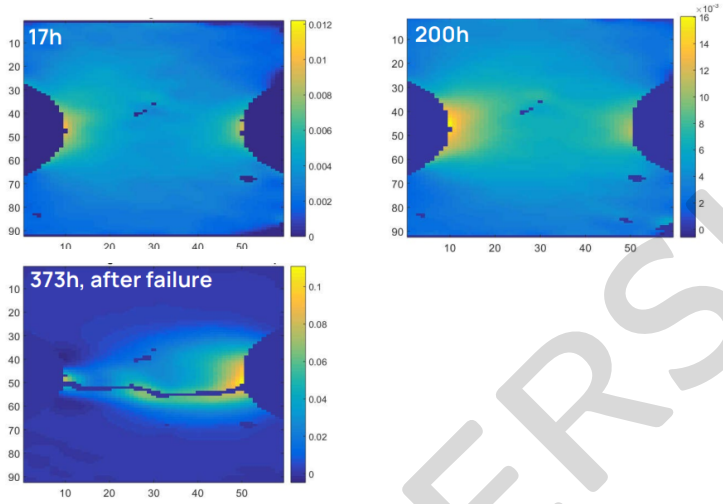

Figure 99

A key aspect of such measurements is that the scale bar used to represent strain magnitudes often changes from one observation to another. This is because localized regions can exhibit strain concentrations orders of magnitude higher than the average bulk strain.
Hence, interpreting experimental creep strain data always requires careful attention to the reference scale, to avoid misestimating the severity of local deformations.

Advanced techniques, such as **Digital Image Correlation (DIC)**, **strain gauges** with fine spatial resolution, or **micro-indentation mapping**, are commonly employed to capture the local creep strain fields.
These techniques reveal how, over prolonged service, strain accumulates preferentially at stress concentrators, leading to damage nucleation and, eventually, crack formation.

4.7.1 Creep Crack Initiation and Growth

In structural components operating under conditions where creep is active, cracks may form and propagate entirely due to time-dependent creep deformation. This phenomenon is distinct from conventional fracture mechanics at lower temperatures, where cracks typically propagate under immediate overload or cyclic fatigue.
For creep, the life of a component threatened by cracking is therefore described by two principal stages:

Creep Crack Initiation (CCI) refers to the period required for a detectable crack to form in a material that is subjected to sustained loading in the creep regime. The initiation time, denoted by t_i, depends strongly on the applied stress, the geometry of the component, the presence of stress concentrators, and the local material microstructure. Creep ductility plays a decisive role here: more ductile materials may accommodate greater strain before cracks form, delaying the initiation phase.

Once a crack has formed, **Creep Crack Growth (CCG)** governs the subsequent propagation. This stage is quantified by the crack growth rate, $\frac{da}{dt}$, which describes how rapidly the crack extends as a function of time. The crack growth rate is not constant but typically increases with the applied load and with the severity of the local stress intensity near the crack tip.

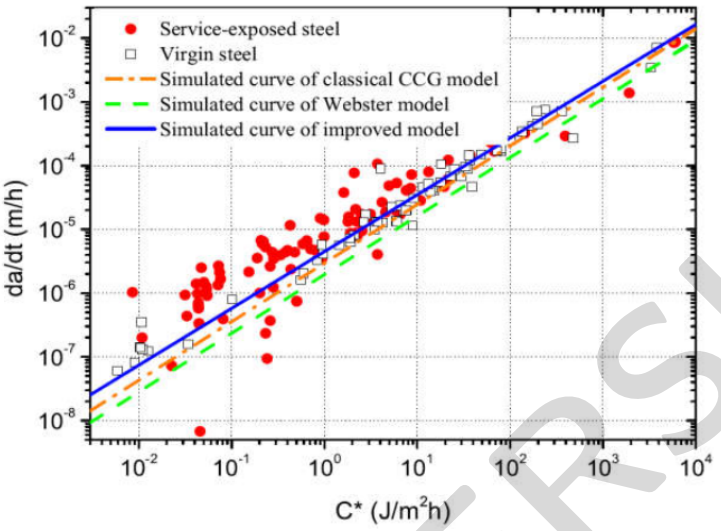

Figure 100

Empirical and theoretical investigations have shown that the creep crack growth rate often displays an approximately linear dependence on a suitable load parameter, such as the stress intensity factor or the **C*-integral** (a parameter used in fracture mechanics to characterize the crack-tip field under creep conditions).

Note

This relationship can be visualized in a typical graph where the crack growth rate $\frac{da}{dt}$ is plotted against the applied load parameter, showing a clear trend of increasing propagation rate with increasing load.

Key Observations for Complex Components

In practice, real engineering components rarely experience the uniform, simple stress states assumed in standard uniaxial creep tests. Instead, the combination of complex geometries and variable loading conditions leads to significant departures from the behaviour predicted by nominal stress alone.

In the presence of notches or other stress concentrators, the local stress can far exceed the nominal net section stress, resulting in localized creep deformation and damage. This can have markedly different effects depending on whether the material is creep-ductile or creep-brittle.

a) In **creep-ductile materials**, local plasticity and creep deformation tend to redistribute stress concentrations over time, a process known as creep strengthening.
Here, the material's capacity for time-dependent plastic flow allows stress relaxation near notches, delaying damage accumulation and extending service life relative to what would be predicted under uniaxial stress.

b) Conversely, in **creep-brittle materials**, the local accumulation of microstructural damage – such as voids and microcracks – limits the effectiveness of stress redistribution.